Available online at www.sciencedirect.com

SCIENCE DIRECT®

ELSEVIER

International Journal of Heat and Mass Transfer 48 (2005) 3244–3252

International Journal of HEAT and MASS TRANSFER

www.elsevier.com/locate/ijhmt

Comparison of dynamic performance for direct and fluid coupled indirect heat exchange systems

N.M. Rao [a,*], B. Maiti [b], P.K. Das [b]

[a] Department of Mechanical Engineering, Dr. Babasaheb Ambedkar Technological University, 'Vidyavihar', Lonere 402 103 Maharashtra State, India

[b] Department of Mechanical Engineering, Indian Institute of Technology, Kharagpur 721 302, West Bengal, India

Received 11 August 2004

Abstract

Three different arrangements of heat exchange from a hot fluid stream to a cold fluid stream such as, direct heat exchanger and fluid coupled indirect heat exchanger both with forced circulation loop as well as thermally driven natural circulation loop have been considered in the present work. Dynamic performance of these three arrangements has been studied for four different excitations namely, step, ramp, exponential and sinusoidal. These excitations are imposed at the hot fluid inlet temperature. Finite element technique is used to solve the transient one-dimensional conservation equations. A thorough comparison of the dynamic performance of these three arrangements is made. It is found that the direct heat exchanger does not have any time delay between the response and the excitation function. Moreover, the phase difference between the sinusoidal excitation and response is the lowest in this case.

Keywords: Direct heat exchanger; Fluid coupled indirect heat exchanger; FCL; NCL; Dynamic performance; FEM

1. Introduction

Exchange of thermal energy between two fluid streams is a very common requirement in different industrial processes. This need has been the motivating force for the evolution of a multitude variety of heat exchangers. There are two main variations of heat exchanger design. In a recuperator, direct and continuous transfer of thermal energy takes place between the two fluids. On the other hand, in a regenerator thermal energy is transported from one fluid to another through an intermediate thermal medium in the form of a solid matrix. However, in certain applications it may not be possible to bring the two fluid streams in close proximity. This may be due to the typical plant design or process requirement or to avoid the contamination between the two fluids. In these typical situations, the transfer of thermal energy is still possible through an intermediate fluid called 'coupling fluid'. Thus, these heat exchange systems are termed as fluid coupled indirect heat exchange systems or simply fluid coupled indirect heat exchangers (FCHE). The concept of fluid coupled indirect heat exchangers has been explained by London and Kays [1]. Further, the work on fluid coupled indirect

* Corresponding author. Tel.: +91 2140 275228(R)/ 275034(O); fax: +91 2140 275040.

E-mail addresses: nmuralidhararao@yahoo.com (N.M. Rao), bmaiti@mech.iitkgp.ernet.in (B. Maiti), pkd@mech.iitkgp.ernet.in (P.K. Das).

0017-9310/$ - see front matter © 2005 Elsevier Ltd. All rights reserved.
doi:10.1016/j.ijheatmasstransfer.2005.02.021

Nomenclature

A_s	cross-sectional area, m^2
c	specific heat, kJ/kg K
C	heat capacity rate, kW/K
C^*	non-dimensional heat capacity rate, $\left(\frac{C}{(\mu cD)_{\mathrm{cf}}}\right)$ or $\left(\frac{C}{(\mu cD)_{\mathrm{c}}}\right)$
D	loop diameter, m
g	gravitational acceleration, m/s^2
Gr_{L}	loop Grashof number, dimensionless, $\left(\frac{\rho_0^2 g\beta D^3(T_0-T_{\mathrm{ci}})}{\mu_{\mathrm{cf}}^2}\right)$
K_1	ratio of vertical to horizontal length of the loop, dimensionless
K_2	ratio of horizontal length to diameter of the loop, dimensionless
L_1	horizontal length of the loop/direct heat exchanger, m
L_2	vertical length of the loop, m
Ntu_{c}	$(UA)_{\mathrm{c}}/C_{\mathrm{min,c}}$ (CEHE), dimensionless
Ntu_{h}	$(UA)_{\mathrm{h}}/C_{\mathrm{min,h}}$ (HEHE), dimensionless
Ntu_{t}	$(UA)_{\mathrm{t}}/C_{\mathrm{min}}$ (DHE), dimensionless
Ntu_{c}^*	$(UA)_{\mathrm{c}}^*/C_{\mathrm{c}}^*$, dimensionless
Ntu_{h}^*	$(UA)_{\mathrm{h}}^*/C_{\mathrm{h}}^*$, dimensionless
Ntu_{t}^*	$(UA)_{\mathrm{t}}^*/C_{\mathrm{h}}^*$, dimensionless
s	space coordinate, m
S	non-dimensional space coordinate, $\left(\frac{s}{L_1}\right)$
t	time, s
u	velocity, m/s
UA	product of over-all heat transfer coefficient and heat transfer area, kW/K
$(UA)^*$	non-dimensional product of overall heat transfer coefficient and heat transfer area, $\left(\frac{(UA)}{(\mu cD)_{\mathrm{cf}} or (\mu cD)_{\mathrm{c}}}\right)$

Greek symbols

β	thermal expansion coefficient, K^{-1}
θ	non-dimensional temperature, $\left(\frac{(T-T_{\mathrm{ci}})}{(T_0-T_{\mathrm{ci}})}\right)$
μ	viscosity, kg/m s
ρ	density, kg/m^3
τ	non-dimensional time, dimensionless, $\left(t\left[\left(\frac{\mu D}{\rho A_s}\right)_{\mathrm{cf}}\frac{1}{L_1}\right]\right)$ or $\left(t\left[\left(\frac{\mu D}{\rho A_s}\right)_{\mathrm{c}}\frac{1}{L_1}\right]\right)$

Subscripts

c	cold stream
cf	coupling fluid
ci	cold stream inlet
d	delay
h	hot stream
0	reference
t	total

heat exchanger has been carried out by Coppage et al. [2]. Though, FCHE generally gives rise to higher cost, increase in power and space requirements, they have some unique advantages over conventional heat exchangers [1]. Few of them are: the frontal areas for two main fluid streams can be shaped independently; use of a multiplicity of smaller units may simplify manufacture, cleaning and servicing, and, reduce the stress problems arising from thermal expansions; closer approach to counterflow characteristics can be realized without suffering a penalty in shape; and so on.

The fluid coupled indirect heat exchange system consists of two independent heat exchanger units which may be termed as 'hot end heat exchanger' and 'cold end heat exchanger' and flow circuit for the circulation of the coupling fluid. With this arrangement the circulating fluid (coupling fluid) transfers the thermal energy from the hot fluid stream to the cold fluid stream. Circulation of coupling fluid at a desired rate is normally achieved using a pump or any prime-mover. Alternatively, one may operate the loop in natural circulation mode exploiting the density gradient.

In the works of London and Kays [1], and, Coppage et al. [2], the circulation of coupling fluid was forced using a pump. They found the main disadvantage with their arrangement was suitability of 'good' fluid heat transfer medium for coupling the hot and cold end heat exchangers, which was to be handled by a pump. Though, this problem could have been handled well with natural circulation, a little work had been done on natural circulation loops by that time. The concept of natural circulation loop (NCL), sometimes also called thermosyphon, had come in to the limelight only after the pioneering works of Keller [3] and Welander [4]. Thereafter, one can see considerable growth in research on NCLs (thermosyphons), attracting the attention of many authors. One example was the survey monograph of Japikse [5]. The main advantages of these NCLs are: highly self sustained, reliable, quieter in operation, less expensive, no restriction in usage of type of coupling fluid and less chance of contamination and low requirement of make-up fluid. These qualities makes NCLs to stand at the cutting edge of modern research and attraction, and, usage of superior quality of coupling fluid, eliminating the main drawback, which was thought to be unresolved problem in the studies of London and Kays [1], and, Coppage et al. [2]. Therefore, the NCLs are of interest in many different contexts. On one hand, NCLs are being used for cooling of electronic chips, nuclear reactors, internal combustion engines, turbine blades, etc. On the other hand, these are also being used for solar water heaters, space heating, advanced heavy water reactors (AHWR), waste heat recovery systems and so on. In fact, NCLs can be represented by simplified models for natural convection of fluids, which are ubiquitous in nature (atmospheric, oceanic circulation loops, etc.).

The contribution in the present paper is the comparison of dynamic performance for direct heat exchanger, fluid coupled indirect heat exchangers with forced circulation loop (FCL) and fluid coupled indirect heat exchangers with natural circulation loop (NCL) for the identical geometrical, physical and operating conditions. In most of the engineering applications the designer or the operator is concerned about the steady state performance of these three arrangements. However, operation of the heat exchanger (direct or indirect) during the transient case cannot be ruled out during startup, shutdown, control operation, accident and failure. Moreover, often they operate under variable input conditions especially in process plants. It is important to know the performance of the heat exchangers (direct or indirect) under such situation to assess the overall system performance to design the control strategies and to take the different preventive measures for safety. The dynamic performance of direct heat exchangers [Fig. 1(a)] has been studied in detail [6–12].

Works on dynamic behaviour of multistream heat exchangers can also be seen in the literature [13–15]. Multistream heat exchangers are widely used in process industries such as gas processing and petrochemical industries. Luo et al. [16] modelled and simulated the dynamic behaviour of one dimensional flow (cocurrent and countercurrent) multistream heat exchangers and their networks. They have introduced four connection matrices through which the solution becomes general and it could directly be applied to one dimensional flow heat exchanger networks. The responses to inlet temperature and flow rate variations are calculated numerically and for some cases analytically. Examples have taken to illustrate the procedure. One of these is indirect coupled heat exchanger system where, for the circulation of coupling fluid a prime-mover is used. System responses to a unit step disturbance in the temperature as well as mass flow rate of one of the external fluid streams and to a unit step disturbance in the mass flow rate of the circu-

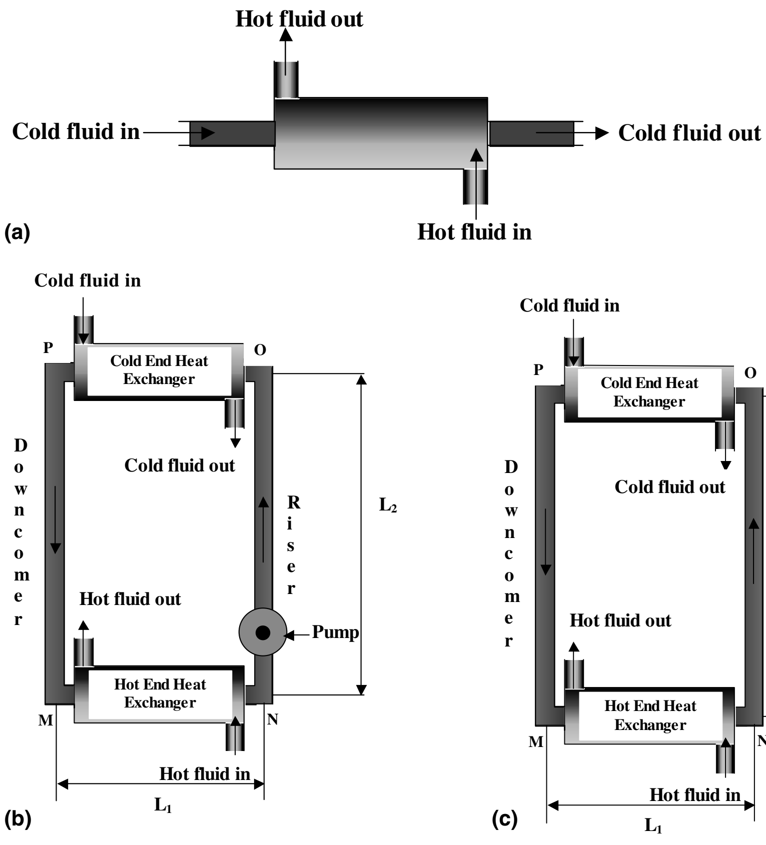

Fig. 1. Different counter current stream arrangements for heat transport: (a) direct heat exchanger; (b) fluid coupled indirect heat exchanger with FCL and (c) fluid coupled indirect heat exchanger with NCL.

lating fluid have been studied. A most general analytical calculation method is presented for systems of counterflow and cocurrentflow heat exchangers by Ranong and Roetzel [17]. They further, extended this method to the FCL system of two coupled heat exchangers. They observed a different transient behaviour than the direct heat exchange systems. This has become more apparent when a perturbation in circulation rate of the coupling fluid is introduced where the outlet temperatures of hot and cold streams subjected to initial oscillations. They observed that the amplitude of these oscillations diminishes gradually and finally reaches a steady-state. These induced temperature oscillations due to perturbation in circulation flow rate did not exist in direct heat exchangers. However, hardly one can find any literature on the dynamic performance of indirect heat exchangers coupled by an NCL.

2. Description of arrangements

In Fig. 1 three different arrangements have been shown for thermal transport between a cold and a hot stream. Fig. 1(a) is a typical counter flow concentric tube heat exchanger where the two streams exchanges energy through the solid wall of the heat exchanger.

Fig. 1(b) and (c) depict fluid coupled indirect heat exchangers. The cold and hot streams exchange the energy through an intermediate fluid stream incorporating two counterflow concentric tube heat exchangers. The coupling fluid absorbs energy from the hot stream in the hot end heat exchanger and transfers it to the cold stream in the cold end heat exchanger.

The difference between the two arrangements arises from the mechanism of circulation of the third or the coupling fluid. In Fig. 1(b) the coupling fluid is circulated with the help of a pump and the arrangement is called forced circulation loop (FCL). On the other hand, in Fig. 1(c) the motion of the coupling fluid is due to thermally driven natural convection. Accordingly, the loop is termed as natural circulation loop (NCL). It may be noted that for exploiting the buoyancy effect, the hot end heat exchanger should be placed below the cold end heat exchanger in the NCL. In FCL, however, no such restrictions are there.

3. Development of mathematical models

To make a uniform basis of comparison, the NCLs and FCLs of fluid coupled heat exchangers have been considered with identical heat exchanger geometry and steady state circulation rate. The product of overall heat transfer coefficient and area in case of direct heat exchanger has been selected carefully so that, its performance can be compared with the other two systems. The analysis is given below. Heat capacities of both hot and cold fluid streams have been kept identical for the three cases. One dimensional analysis has been made for the three systems. Further details have been given in Rao [18] and Rao et al. [19].

4. Fluid coupled indirect heat exchanger with NCL

For analyzing the performance of an NCL one needs to consider the momentum and energy equations for the coupling fluid and the energy equations for the hot and the cold streams. In natural circulation both fluid flow field and temperature profile generates simultaneously during transient operation. As the circulation loop is of uniform cross section the velocity of coupling fluid becomes a function of time only, however, temperature is a function of both time and space during transient condition. The momentum equation for the entire loop, as derived in Rao [18], is written as

$$\frac{2(L_1+L_2)}{(A_sc)_{\mathrm{cf}}}\frac{\partial C_{\mathrm{cf}}}{\partial t}+\frac{4a\mu_{\mathrm{cf}}^b(L_1+L_2)}{\rho_{\mathrm{cf}}(A_sc)_{\mathrm{cf}}^{2-b}}C_{\mathrm{cf}}^{2-b} + \rho_0 g\beta\left[\int_{(2L_1+L_2)}^{2(L_1+L_2)}T_{\mathrm{cf}}\mathrm{d}s-\int_{L_1}^{(L_1+L_2)}T_{\mathrm{cf}}\mathrm{d}s\right]=0. \tag{1}$$

The energy equations for the external fluid stream and the coupling fluid, as deduced in Rao [18], are given below for a differential element.

For hot end heat exchanger

$$\frac{\partial T_{\mathrm{h}}}{\partial t}-u_{\mathrm{h}}\frac{\partial T_{\mathrm{h}}}{\partial s}+\frac{(UA)_{\mathrm{h}}}{(\rho A_sc)_{\mathrm{h}}L_1}(T_{\mathrm{h}}-T_{\mathrm{cf}})=0, \tag{2}$$

$$\frac{\partial T_{\mathrm{cf}}}{\partial t}+u_{\mathrm{cf}}\frac{\partial T_{\mathrm{cf}}}{\partial s}+\frac{(UA)_{\mathrm{h}}}{(\rho A_sc)_{\mathrm{cf}}L_1}(T_{\mathrm{cf}}-T_{\mathrm{h}})=0. \tag{3}$$

For cold end heat exchanger

$$\frac{\partial T_{\mathrm{c}}}{\partial t}-u_{\mathrm{c}}\frac{\partial T_{\mathrm{c}}}{\partial s}+\frac{(UA)_{\mathrm{c}}}{(\rho A_sc)_{\mathrm{c}}L_1}(T_{\mathrm{c}}-T_{\mathrm{cf}})=0, \tag{4}$$

$$\frac{\partial T_{\mathrm{cf}}}{\partial t}+u_{\mathrm{cf}}\frac{\partial T_{\mathrm{cf}}}{\partial s}+\frac{(UA)_{\mathrm{c}}}{(\rho A_sc)_{\mathrm{cf}}L_1}(T_{\mathrm{cf}}-T_{\mathrm{c}})=0. \tag{5}$$

The riser and downcomer are assumed adiabatic. Accordingly, the change of temperature in these sections are given by

$$\frac{\partial T_{\mathrm{cf}}}{\partial t}+u_{\mathrm{cf}}\frac{\partial T_{\mathrm{cf}}}{\partial s}=0. \tag{6}$$

In the present study, excitation has been imposed at the inlet temperature of the hot fluid stream. Therefore, the boundary conditions are

$$T_{\mathrm{h}}(s,t)=T_{\mathrm{h}}(t)\ \text{at}\ s=L_1\ \text{i.e. at a station ‘}\mathbf{N}\text{’} \tag{7}$$

$$T_c(s,t) = T_{ci} \text{ at } s = (2L_1 + L_2) \text{ i.e. at a station '}\mathbf{P}\text{'} \quad (8)$$

The initial conditions are

$$T_{h,c,cf}(s,0) = \text{constant (known temperature) at } s = s \text{ and } t = 0 \quad (9)$$

Momentum and energy equations along with the boundary conditions can be non-dimensionalised by using the following substitutions.

$$C^*_{h,c,cf} = \frac{C_{h,c,cf}}{(\mu c D)_{cf}} \quad (10a)$$

$$(UA)^*_{h,c} = \frac{(UA)_{h,c}}{(\mu c D)_{cf}} \quad (10b)$$

$$\theta_{h,c,cf} = \frac{(T_{h,c,cf} - T_{ci})}{(T_0 - T_{ci})} \quad (10c)$$

$$\tau = t\left[\left(\frac{\mu D}{\rho A_s}\right)_{cf}\frac{1}{L_1}\right] \quad (10d)$$

$$S = \frac{s}{L_1}; \quad K_1 = \frac{L_2}{L_1}; \quad K_2 = \frac{L_1}{D} \quad (10e)$$

$$Ntu^*_{h,c} = \frac{(UA)^*_{h,c}}{C^*_{h,c}} \quad (10f)$$

$$Gr_L = \frac{\rho_0^2 g \beta D^3 (T_0 - T_{ci})}{\mu_{cf}^2} \quad (10g)$$

Using the above non-dimensional parameters Eqs. (1)–(6) can be represented as (11)–(16) respectively.

$$\frac{\partial C^*_{cf}}{\partial \tau} + \frac{\pi^b a K_2}{2^{2b-1}}(C^*_{cf})^{2-b} + \frac{\pi^2}{2^5} Gr_L K_2 \frac{1}{(1+K_1)} \times \left[\int_{(K_1+2)}^{2(K_1+1)} \theta_{cf}\,dS - \int_1^{(K_1+1)} \theta_{cf}\,dS\right] = 0 \quad (11)$$

$$\frac{\partial \theta_h}{\partial \tau} - C^*_h R_h \frac{\partial \theta_h}{\partial S} + Ntu^*_h C^*_h R_h(\theta_h - \theta_{cf}) = 0 \quad (12)$$

$$\frac{\partial \theta_{cf}}{\partial \tau} + C^*_{cf} \frac{\partial \theta_{cf}}{\partial S} + Ntu^*_h C^*_h(\theta_{cf} - \theta_h) = 0 \quad (13)$$

$$\frac{\partial \theta_c}{\partial \tau} - C^*_c R_c \frac{\partial \theta_c}{\partial S} + Ntu^*_c C^*_c R_c(\theta_c - \theta_{cf}) = 0 \quad (14)$$

$$\frac{\partial \theta_{cf}}{\partial \tau} + C^*_{cf} \frac{\partial \theta_{cf}}{\partial S} + Ntu^*_c C^*_c(\theta_{cf} - \theta_c) = 0 \quad (15)$$

$$\frac{\partial \theta_{cf}}{\partial \tau} + C^*_{cf} \frac{\partial \theta_{cf}}{\partial S} = 0 \quad (16)$$

where, $R_{h,c} = \frac{(\rho A_s c)_{cf}}{(\rho A_s c)_{h,c}}$ ratio of coupling fluid heat capacitance to hot/cold stream heat capacitance per unit length.

The boundary conditions in the non-dimensional form are

$$\theta_h(S,\tau) = \theta_h(\tau) \text{ at } S = 1.0 \quad (17)$$

$$\theta_c(S,\tau) = 0.0 \text{ at } S = (K_1 + 2) \quad (18)$$

The non-dimensional initial conditions are

$$\theta_{h,c,cf}(S,\tau) = 0.0 \text{ at } S = S \quad \text{and } \tau = 0 \quad (19)$$

5. Fluid coupled indirect heat exchanger with FCL

In this arrangement, a pump or any suitable device is used to provide fluid flow at the desired rate. Hence, one can find only development of coupling fluid temperature profile in transient condition. Therefore, the energy equations (2)–(6) and (12)–(16) are to be considered in dimensional and non-dimensional forms, respectively, in this case. Further, identical boundary and initial conditions have been considered [Eqs. (7)–(9) in dimensional and (17)–(19) in non-dimensional forms].

6. Direct heat exchanger

The energy balance equation for a hot stream and a cold stream considering a differential element of direct heat exchanger can be written, respectively, as,

$$\frac{\partial T_h}{\partial t} - u_h \frac{\partial T_h}{\partial s} + \frac{(UA)_t}{(\rho A_s c)_h L_1}(T_h - T_c) = 0, \quad (20)$$

$$\frac{\partial T_c}{\partial t} + u_c \frac{\partial T_c}{\partial s} + \frac{(UA)_t}{(\rho A_s c)_c L_1}(T_c - T_h) = 0. \quad (21)$$

The boundary and initial conditions are similar to other two arrangements.

The above equations can be non-dimensionalised by using the following substitutions.

$$C^*_{h,c} = \frac{C_{h,c}}{(\mu c D)_c} \quad (22)$$

$$(UA)^*_t = \frac{(UA)_t}{(\mu c D)_c} \quad (23)$$

$$\theta_{h,c} = \frac{(T_{h,c} - T_{ci})}{(T_0 - T_{ci})} \quad (24)$$

$$S = \frac{s}{L_1} \quad (25)$$

$$\tau = t\left[\left(\frac{\mu D}{\rho A_s}\right)_c \frac{1}{L_1}\right] \quad (26)$$

Though, the non-dimensionalisation of $C^*_{h,c}$, $(UA)^*_t$ and τ have been performed on the basis of $(\mu c D)_c$, identical values of $C^*_{h,c}$, $(UA)^*_t$ and τ have been used for the comparison of three arrangements.

Using the above non-dimensionalisation, Eqs. (20) and (21) can be represented as follows:

$$\frac{\partial\theta_h}{\partial\tau} - C^*_h R\frac{\partial\theta_h}{\partial S} + Ntu^*_t C^*_h R(\theta_h - \theta_c) = 0 \quad (27)$$

$$\frac{\partial\theta_c}{\partial\tau} + C^*_c\frac{\partial\theta_c}{\partial S} + Ntu^*_t C^*_h(\theta_c - \theta_h) = 0 \quad (28)$$

where

$$Ntu^*_t = \frac{(UA)^*_t}{C^*_h} \quad (29)$$

and $R = \frac{(\rho A_s c)_c}{(\rho A_s c)_h}$, ratio of the cold stream heat capacitance to hot stream heat capacitance per unit length.

For comparing the dynamic behaviour of the three possible heat exchange arrangements, the $(UA)^*_t$ has been taken as,

$$(UA)^*_t = [(UA)^*_h + (UA)^*_c]. \quad (30)$$

where, $(UA)^*_h$ and $(UA)^*_c$ are the product of overall heat transfer coefficient and area of hot and cold end heat exchangers, respectively, for both FCLs and NCLs. As $Ntu_{h,c}* = \frac{(UA)_{h,c}*}{C_{h,c}*}$ is derived in Eq. (10f) $(UA)^*_h$ and $(UA)^*_c$ can be expressed as

$$(UA)^*_h = Ntu^*_h C^*_h \quad \text{and} \quad (UA)^*_c = Ntu^*_c C^*_c. \quad (31)$$

On substitution of Eq. (31) into Eq. (30) yields

$$(UA)^*_t = [Ntu^*_h C^*_h + Ntu^*_c C^*_c] \quad (32)$$

Therefore, Ntu^*_t may become by substituting Eq. (32) into Eq. (29) written

$$Ntu^*_t = \left[Ntu^*_h + \left(Ntu^*_c\frac{C^*_c}{C^*_h}\right)\right] \quad (33)$$

For the present study, the hot and cold stream heat capacities are taken as identical ($C^*_h = C^*_c$). This gives

$$Ntu^*_t = [Ntu^*_h + Ntu^*_c] \quad (34)$$

The chosen numerical values for Ntu^*_h and Ntu^*_c are 5 and 2, respectively. Hence, the numerical value for Ntu^*_t becomes 7 and same is taken while comparing the three arrangements. Moreover, as R is also equal to the ratio of R_h to $R_c(\frac{(\rho A_s c)_{cf}}{(\rho A_s c)_h} / \frac{(\rho A_s c)_c}{(\rho A_s c)_{cf}} = \frac{(\rho A_s c)_c}{(\rho A_s c)_h})$, its numerical value also becomes the ratio of these two. Since, numerical values of R_h and R_c have taken as 5000 and 1000, respectively; $R = 5$.

7. Solution methodology

For the evaluation of the dynamic performance of these three arrangements, a finite element technique is used. Eqs. (11)–(16) are coupled in nature and required to be solved simultaneously. Same computational code based on finite element technique with modifications according to the type of arrangement is used to determine the dynamic performance of all three arrangements. The detailed numerical solution based on finite element method (FEM) can be obtained from Rao [18] and Rao et al. [19].

Four types of excitations namely, step, ramp, exponential and sinusoidal have been considered and applied at the inlet of hot fluid inlet temperature. The maximum temperature limit imposed to the step function is 1.0. The ramp and exponential functions considered in the present work are to some extent different from those used by the earlier researchers [20,21,9], etc. Conventionally, a continuous increase in the functional value with time is considered for both ramp and exponential functions. This is unlikely in a real situation. The ramp and exponential functions are modified such that the maximum functional values are limited to 1.0. It may be noted that a pure step function can also not be realized in practice. Rather, the maximum functional value may be reached by a steep slope. This can be represented by the modified ramp function considered in the present work. Further, the amplitude for the sinusoidal function is also restricted to 1.0. The final expressions for these excitations have been given below

$$\theta_h(\tau) = \begin{cases} 1 & \text{for step input} \\ \begin{bmatrix} \alpha\tau, & \tau \leqslant \alpha^{-1} \\ 1, & \tau > \alpha^{-1} \end{bmatrix} & \text{for ramp input} \\ 1 - e^{-\alpha\tau} & \text{for exponential input} \\ [0.75 + (0.25\sin\alpha\tau)] & \text{for sinusoidal input} \end{cases} \quad (35)$$

The input signals are schematically represented in Fig. 2. For the present study, α has been taken as 500 for ramp input and 5000 for exponential input. For the sinusoidal excitation the value of 'α' has been taken as 5000.

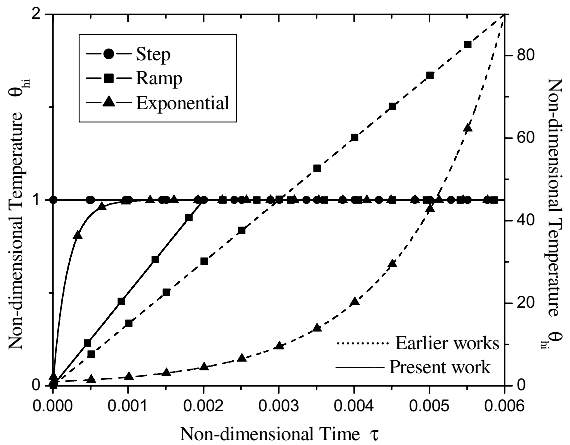

Fig. 2. Schematic representation of the input signals.

8. Results and discussion

Fig. 3 depicts the response of the cold stream exit temperature for a step input to the hot stream inlet temperature for the three different arrangements of heat exchange shown in Fig. 1. It is interesting to note that, the responses in the three cases are substantially different from each other. In case of direct heat exchanger there is no time delay for the cold stream temperature. The cold stream exit temperature starts rising immediately from the initiation of the step input. The steady state temperature at the exit of the cold stream is also the highest in this case. This is because the cold stream absorbs heat directly from the hot stream, so it can approach the hot stream temperature closely. The maximum time delay is observed in case of NCL as the cold stream will sense the effect of input excitation only after the flow field has developed inside the loop. Moreover, the cold stream exit temperature goes through an oscillation of diminishing frequency before attaining the steady state value. During the start up of the NCL form its frozen state a series of coupled thermal–hydraulic phenomena takes place. Initially, as there is no fluid flow the temperature of coupling fluid in contact with the hot end heat exchanger increases to a high value where as the fluid temperature at the top of the loop remains at its initial value. This creates a large buoyancy force and hence stronger circulation. However, with the development of circulation the fluid temperature leaving the heating section decreases. This causes a fall in the circulation rate. The oscillation in θ_{co} is an outcome of the variation in circulation rate and the change of fluid temperature at point 'O' of the loop [Fig. 1(c)]. This phenomenon is discussed in detail in Rao [18]. For FCL the time delay will have an intermediate value. Though the flow field is established in an FCL a finite time taken for the transport of thermal energy is responsible for this delay.

The time delay 'τ_d' is derived below for NCL. Considering the motion of a fluid particle through the riser one may write

$$\mathrm{d}s_{\mathrm{riser}} = u_{\mathrm{cf}}\,\mathrm{d}t. \tag{36}$$

Therefore

$$\int_0^{L_2} \mathrm{d}s_{\mathrm{riser}} = \int_0^{t_d} u_{\mathrm{cf}}\,\mathrm{d}t \tag{37}$$

The above Eq. (37) may be written in non-dimensional form

$$\int_1^{(1+K_1)} \mathrm{d}S = \int_0^{\tau_d} C^*_{\mathrm{cf}}\mathrm{d}\tau. \tag{38}$$

Therefore

$$K_1 = \int_0^{\tau_d} C^*_{\mathrm{cf}}\mathrm{d}\tau. \tag{39}$$

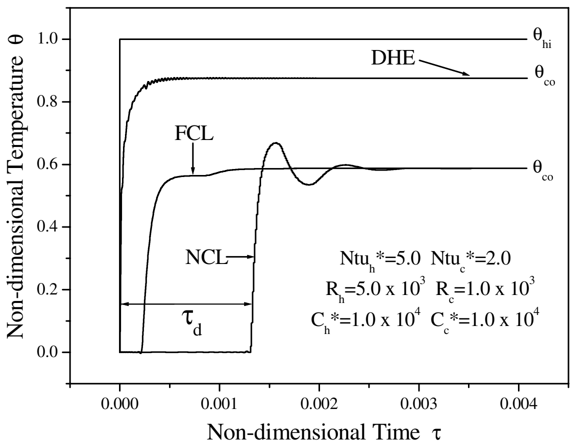

Fig. 3. Exit responses of cold stream to step change in hot stream inlet temperature.

The value of τ_d obtained by numerical integration of Eq. (39), exactly matches with its value obtained from the temperature response curve [Fig. 3]. In case of FCL also the time delay can be calculated using Eq. (39). However, C^*_{cf} is constant in this case and can be taken out of the integration sign:

$$\tau_d = \frac{K_1}{C^*_{\mathrm{cf}}} \tag{40}$$

In case of NCL C^*_{cf} increases starting from zero value, whereas C^*_{cf} has a non-zero finite value (steady-state value) in case of FCL. This explains the difference in time delay in these two cases. Moreover, in case of FCL there is no appreciable fluctuation in the response of the cold stream exit temperature and its steady state value will be equal to that of NCL.

The general nature of the response for modified ramp and exponential excitation (Figs. 4 and 5) is similar to

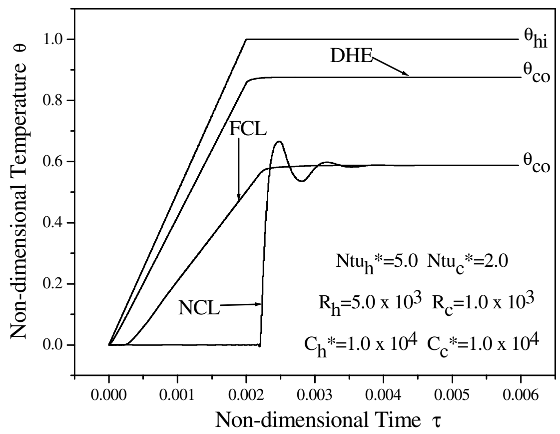

Fig. 4. Exit responses of cold stream to ramp change in hot stream inlet temperature.

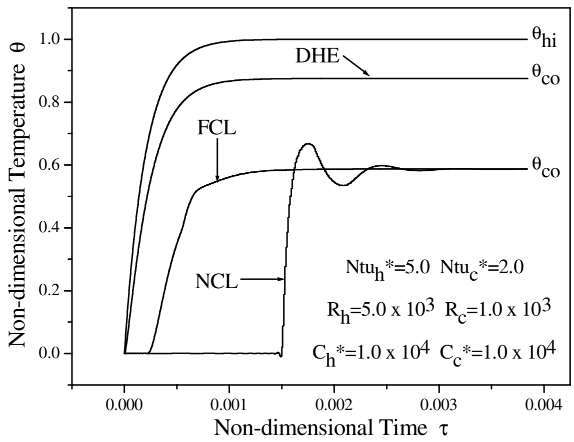

Fig. 5. Exit responses of cold stream to exponential change in hot stream inlet temperature.

that of step input. In both of these cases the cold fluid exit temperature will be highest in a direct heat exchanger. NCL will exhibit a steep rise of cold fluid temperature with the largest value of time delay. Like the step input the cold stream exit temperature will also go through some oscillations before reaching the steady-state for ramp and exponential inputs. The temperature response curves of the FCL will start with the pattern of input excitation.

Finally, Fig. (6) depicts the response of the three energy exchange systems for sinusoidal input excitation. The cold stream exit temperature from all the three systems shows sinusoidal variations once the steady state is reached. The frequency of the variation is equal to that of the input excitation. However, the temperature variation from the direct heat exchanger has the highest average temperature as well as the highest amplitude. All the output curves depict a phase shift with input excitation. The phase shift is minimum in case of direct heat exchanger.

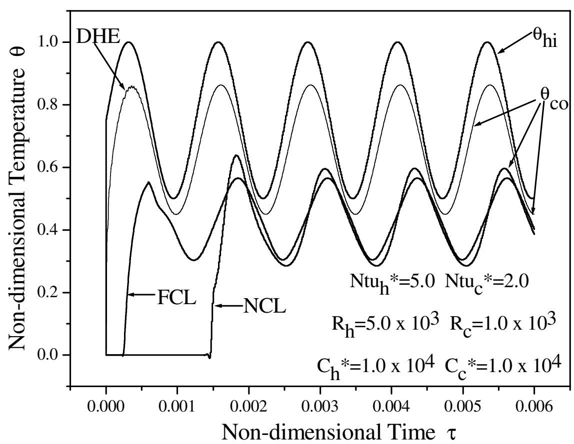

Fig. 6. Exit responses of cold stream to sinusoidal change in hot stream inlet temperature.

9. Conclusion

The present study is taken up to compare the dynamic performance of three possible arrangements for the heat transport from hot fluid stream to cold fluid stream. These arrangements are direct heat exchanger, fluid coupled indirect heat exchanger with FCL and fluid coupled indirect heat exchanger with NCL. One-dimensional governing equations have been derived for three arrangements in partial differential form. These equations are coupled in nature particularly for NCL. A finite element technique has been used to solve these equations in transient condition. Four types of excitations are imposed at the inlet temperature of hot fluid stream. These are step, ramp, exponential and sinusoidal excitations. Identical geometrical, operating, boundary and initial conditions have been adopted for the comparison of these three arrangements. It is observed that there is no time delay in case of direct heat exchanger and more time delay in case of NCL. The steady state exit temperature of the cold stream is higher in case of direct heat exchanger and lower and same in FCL and NCL. No appreciable initial oscillations have been observed in DHE as well as in FCL. In case of sinusoidal excitation all output curves of cold fluid outlet temperature show a phase shift and same frequency of input excitation. However, the phase shift is minimum in case of DHE.

References

[1] A.L. London, W.M. Kays, The liquid coupled indirect-transfer regenerator for gas turbine plants, ASME J. Heat Transfer 73 (1951) 529–540.

[2] J.E. Coppage, A.L. London, The periodic-flow regenerator—a summary of design theory, Trans. ASME (1953) 779–787.

[3] J.B. Keller, Periodic oscillations in a model of thermal convection, J. Fluid Mech. 26 (1966) 599–606.

[4] P. Welander, On the oscillatory instability of a differentially heated fluid loop, J. Fluid Mech. 29 (1967) 17–30.

[5] D Japikse, Advance in thermosyphon technologyAdvances in Heat Transfer, 9, Academic Press, New York, 1973, pp. 1–111.

[6] F.E. Romie, Transient response of the counterflow heat exchanger, ASME J. Heat Transfer 106 (1984) 620–626.

[7] F.E. Romie, Transient response of the parallel-flow heat exchanger, ASME J. Heat Transfer 107 (1985) 727–730.

[8] D.D. Gvozdenac, Analytical solution of transient response of gas-to-gas parallel and counterflow heat exchangers, ASME J. Heat Transfer 109 (1987) 848–855.
[9] W. Roetzel, Y. Xuan, Transient response of parallel and counterflow heat exchangers, ASME J. Heat Transfer 114 (1992) 510–512.
[10] P.J. Heggs, C.L. Render, Transient response of heat exchangers with one infinite capacitance fluid, Heat Transfer Eng. 4 (2) (1983) 19–27.
[11] G. Pagliarini, G.S. Barozzi, Thermal coupling in laminar flow double- pipe heat exchangers, ASME J. Heat Transfer 113 (1991) 526–533.
[12] M.A. Abdelghani-Idrissi, F. Bagui, L. Estel, Analytical and experimental response time to flow rate step along a counterflow double pipe heat exchanger, Int. J. Heat Mass Transfer 44 (2001) 3721–3730.
[13] W. Roetzel, Y. Xuan, Dynamic Behaviour of Heat Exchangers, WIT Press, Boston, 1999.
[14] H. Pingaud, J.M. Le Lann, B. Koehret, Steady-state and dynamic simulation of plate fin heat exchangers, Comput. Chem. Eng. 13 (4–5) (1989) 577–585.
[15] W. Roetzel, M. Li, X. Luo, Dynamic behaviour of heat exchangers, in: Seventh International Conference on Advanced Computational Methods in Heat Transfer, April 22–24, 2002, Halkidiki, Greece.
[16] X. Luo, X. Guan, M. Li, W. Roetzel, Dynamic behaviour of one-dimensional flow multistream heat exchangers and their networks, Int. J. Heat Mass Transfer 46 (2003) 705–715.
[17] Ch. Na Ranong, W. Roetzel, Steady state and transient behaviour of two heat exchangers coupled by a circulating flowstream, Int. J. Therm. Sci. 41 (2002) 1029–1043.
[18] N.M. Rao, Investigations on buoyancy induced circulation loops, Ph.D. Thesis, Indian Institute of Technology, Kharagpur, 2002.
[19] N.M. Rao, B. Maiti, P.K. Das, Pressure variation in a natural circulation loop with end heat exchangers, Int. J. Heat Mass Transfer 48 (2005) 1403–1412.
[20] W. Roetzel, Y. Xuan, Transient behaviour of multipass shell-and-tube heat exchangers, Int. J. Heat Mass Transfer 35 (1992) 703–710.
[21] J.C. Daniel, J.L. Marchetti, Dynamic simulation of shell-and-tube heat exchangers, Heat Transfer Eng. 8 (1987) 50–59.